

ORIGINAL RESEARCH ARTICLE

First-Principles Study of the Structural, Mechanical, and Electronic Properties of Ba_3AsCl_3 Perovskite for Optoelectronics and Solar Cell Applications

Yusra Sade Abdullahi^{*1,2} , Garba Babaji² , Abdullahi Lawal³ , Abdulkadir S. Gidado² ¹Department of Physics, Umaru Musa Yar'adua University, Katsina, Katsina State, Nigeria²Department of Physics, Bayero University Kano, Kano State, Nigeria³Department of Physics, Ahmadu Bello University, Zaria, Kaduna State, Nigeria

ABSTRACT

Inorganic lead-free halide perovskites with the A_3BX_3 structure have recently attracted considerable attention in recent years due to their excellent optoelectronic properties. Ba_3AsCl_3 , a pnictogen-based inorganic halide perovskite, emerges as a promising candidate owing to the chemical stability of barium-based crystal structures and the potential of arsenic-derived compounds to exhibit favourable electronic structures. This study presents a detailed first-principles calculation of the structural, elastic, mechanical, and electronic properties of Ba_3AsCl_3 inorganic lead-free perovskite using the Quantum Espresso code. The generalized gradient approximation (GGA) with Perdew–Burke–Ernzerhof (PBE) functional was used to determine the electron exchange and correlation energy. Geometry optimization and variable-cell relaxation verify the stability of the compound in its cubic phase with an optimized lattice parameter of 6.49 Å. This is in good agreement with available theoretical data. The calculated elastic constants indicate that Ba_3AsCl_3 is mechanically stable with a shear modulus of 16.03 GPa, a Young modulus of 40.01 GPa, and a bulk modulus of 27.01 GPa. The calculated machinability index, Hardness, and anisotropy index indicate that Ba_3AsCl_3 has a high machinability index, moderately hard and anisotropic in nature, while Poisson's ratio of 0.251 and the negative value of the Cauchy pressure indicate that it is slightly brittle in nature. Electronic properties investigation reveals that Ba_3AsCl_3 is a direct band gap semiconductor with a band gap value of 0.934 eV (with SOC) and 0.976 eV (without SOC). The density of states (DOS) and PDOS show the conduction band minimum, and the valence band maximum located along the high symmetry point Γ , and the contributions of the orbitals in the electronic state. Ba_3AsCl_3 's bandgap enables near-infrared absorption and efficient charge generation. Overall, this study offers valuable insights into the properties of Ba_3AsCl_3 , suggesting potential for optoelectronics and solar cell applications.

ARTICLE HISTORY

Received June 29, 2025

Accepted December 18, 2025

Published December 30, 2025

KEYWORDS

Perovskites, Ba_3AsCl_3 , DFT, Optoelectronics, Solar Cell.

© The Author(s). This is an Open Access article distributed under the terms of the Creative Commons Attribution 4.0 License [creativecommons.org](https://creativecommons.org/licenses/by-nc/4.0/)

INTRODUCTION

With the increasing global energy demand and growing concerns over environmental degradation, the shift toward renewable energy has become necessary. Among the various alternatives, solar energy is notable for its wide availability and sustainability (Gayen et al., 2024; Shahzad, 2012; Ukoba et al., 2024). Consequently, significant research efforts have focused on improving solar energy conversion technologies. Although many materials have been developed for solar cell technology, achieving low-cost, non-toxic, abundant, and efficient solar cell materials remain challenging for researchers (Lawal et al., 2021).

Perovskite solar cells have attracted significant attention due to their exceptional light-absorption properties and ease of fabrication. The rapid advancement in optoelectronics, particularly in the development of high-

performance solar cells and photodetectors, has been fuelled by the outstanding properties of perovskite materials (Zhang et al., 2023). These materials show real potential for utilization in photodetectors, solar cells, and light-emitting diodes, achieving efficiencies and performance levels that are close to or exceed those of traditional semiconductors. However, the adoption of lead-based perovskites is limited by toxicity concerns in the field of solar cell applications (Hasan et al., 2023). The effects associated with lead-based perovskite have caused immense worry due to the severe environmental contamination it can cause, posing risks to human well-being and environmental sustainability (Ravi et al., 2020).

To address these concerns and move towards more sustainable alternatives, extensive research has shifted

Correspondence: Yusra Sade Abdullahi. Department of Physics, Umaru Musa Yar'adua University, Katsina, Katsina State, Nigeria. ✉ yusra.sade@umyu.edu.ng

How to cite: Sade, Y. A., Babaji, G., Lawal, A., & Gidado, A. S. (2025). First-Principles Study of the Structural, Mechanical, and Electronic Properties of Ba_3AsCl_3 Perovskite for Optoelectronics and Solar Cell Applications. *UMYU Scientifica*, 4(4), 82 – 87. <https://doi.org/10.56919/usci.2544.008>

towards developing lead-free, nontoxic, and eco-friendly substitutes. These lead-free materials retain the desirable structural and optoelectronic properties of traditional lead-based perovskites, but without the environmental hazards (López-Fernández et al., 2024; Pecunia et al., 2020). In recent years, studies have shown that lead-free perovskites with structure A_3BX_3 possess direct band gaps with outstanding optical absorption characteristics, making them suitable for application in solar cells and optoelectronics. Barman et al. (2023) studied the electronic, optical, and mechanical properties of Ba_3AsI_3 using Density functional Theory. Their investigations reveal that this compound is ideal for optoelectronic applications. DFT calculations were also performed by Harun-Or-Rashid et al. (2024) to investigate the properties of lead-free Mg_3SbX_3 . They reported that the compounds have semiconducting behaviour with direct band gaps, making them suitable for solar cell applications. Other A_3BX_3 perovskites, such as Sr_3AsI_3 , Ca_3PI_3 , and Ca_3AsI_3 , have been studied and reported to exhibit excellent optical and electronic properties (Apurba et al., 2024; Rahman et al., 2024). Notable characteristics of these perovskites include strong light absorption, good carrier diffusion lengths, and efficient charge transport.

Among the A_3BX_3 family, Ba_3AsCl_3 is a promising lead-free candidate due to the enhanced chemical stability typically associated with chloride-based perovskites and the favorable ionic radii of Ba and As for stabilizing the A_3BX_3 framework. Despite these advantages, the properties of Ba_3AsCl_3 remain largely unexplored with respect to a comprehensive first-principles analysis that explicitly incorporates Spin-orbit coupling. In this study, we investigate the structural, electronic, elastic, and mechanical properties of Ba_3AsCl_3 using first-principles calculations.

MATERIALS AND METHODS

First Principles computations utilizing density functional theory (DFT) were carried out using Quantum Espresso (Giannozzi et al., 2009) and Thermo PW to investigate the structural, elastic, mechanical and electronic properties of Ba_3AsCl_3 . The exchange-correlation energy is determined using the Generalized Gradient Approximation (GGA) with the Perdew-Burke-Ernzerhof (PBE) functional, while the projected augmented wave (PAW) pseudopotential from the standard solid-state pseudopotential library (Dal Corso, 2014) is employed to treat the electron-ion core interactions. A Convergence test is performed by carrying out self-consistent field calculations with different cutoff energies and Monkhorst-Pack k-point grids. To ensure calculation accuracy, a Cutoff energy of 70 Ry and a $10 \times 10 \times 10$ k-point grid are used to sample the Brillouin zone. For structural properties, we performed a full relaxation of atomic positions and unit-cell dimensions to obtain an optimized lattice constant. Electronic properties were calculated using the self-consistent field (SCF) method, followed by non-self-consistent calculations with a denser $20 \times 20 \times 20$ k-point grid to obtain the band structure (with and without SOC), density

of states, and partial density of states. Elastic constant calculation is carried out by applying a small deformation to relax the structure; the resulting stresses are analyzed to determine the elastic constant (Jamal et al., 2014). These elastic constants serve as the basis for determining several other elastic properties, as well as mechanical properties.

RESULTS AND DISCUSSION

Structural properties

In studying material properties, it is important to start with structural properties, as they serve as a basis for analyzing material characteristics. The structure Ba_3AsCl_3 is a cubic perovskite of the A_3MX_3 type, with space group Pm-3m. Each unit cell contains seven atoms: three Ba, one As, and three Cl (AL-Shomar et al., 2024; Barman et al., 2023; Harun-Or-Rashid et al., 2024). Fig 1 shows the crystal structure and the crystallographic directions of Ba_3AsCl_3 . The lattice parameters of the perovskites calculated are shown in Table 1.

Table 1: Structural parameters of Ba_3AsCl_3

Structural Parameter	Calculated Value
Lattice constant (Å): GGA-PBE	6.26
GGA-PBE+SOC	6.49
Reported lattice constant (Å)	6.51
Volume (Å ³)	273.36
Atoms/unit cell	7

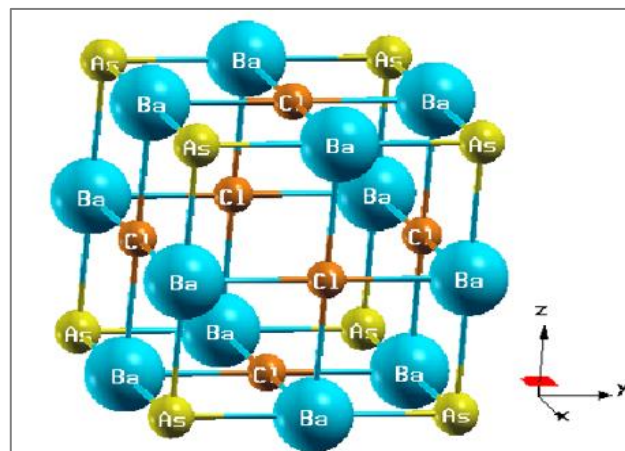


Fig. 1: Crystal structure and crystallographic direction of Ba_3AsCl_3 .

The calculated lattice constant of Ba_3AsCl_3 is consistent with previous work. The value obtained in the absence of SOC is 6.26 Å, which differs by 0.25 Å, approximately 3.8% from the reported value of 6.51 (Feng & Zhang, 2021). After applying spin-orbit coupling (SOC), the calculated lattice parameter shows excellent consistency with a deviation of 0.02 Å, approximately 0.3%. This highlights the importance of SOC in predicting the lattice parameter of Ba_3AsCl_3 .

Electronic properties

Electronic property calculations are crucial for understanding and predicting the optoelectronic properties of materials (Lawal et al., 2017). In this study,

we conduct an in-depth analysis of the electronic properties of Ba_3AsCl_3 . The electronic band structure, density of states, and projected density of states are the electronic properties calculated in this paper. An important concept in condensed matter physics for explaining various properties of materials is the band structure (Barman et al., 2023; Hummel, 2000). The electronic band structure of Ba_3AsCl_3 along high-symmetry points of the Brillouin zone is computed with

and without the addition of spin-orbit coupling (SOC). This is done because of the significant atomic numbers of Ba, As and Cl. Fig. 2(a) and (b) illustrate the electronic band structure of Ba_3AsCl_3 , both with and without consideration of SOC. The red-dashed line indicates the Fermi energy level, set to 0 eV on the energy scale. Based on our band structure calculations, the energy gap between the conduction band minimum and the valence band maximum occurred at the Γ point.

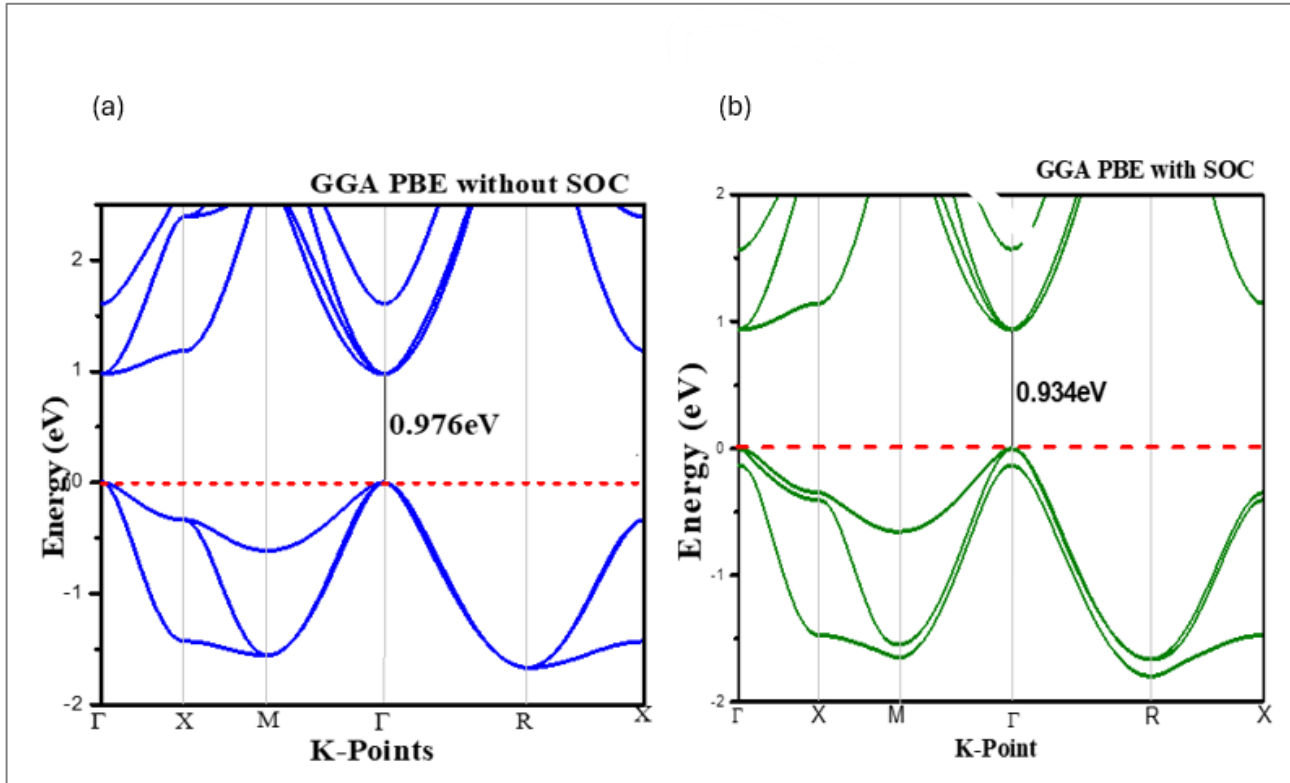


Fig.2: Band structure of Ba_3AsCl_3 (a) without and (b) with SOC

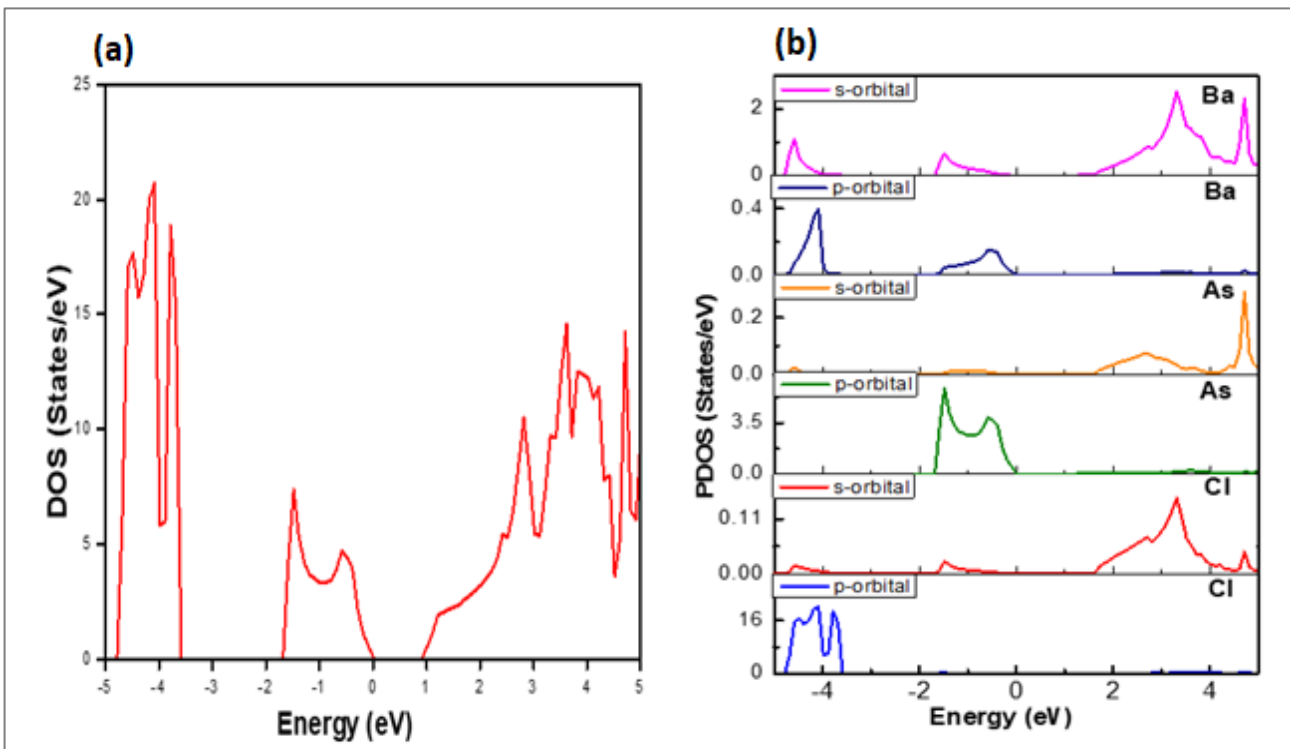


Fig.3: (a) Density of states (DOS), (b) PDOS for Ba_3AsCl_3

This suggests that Ba_3AsCl_3 is a direct-band-gap semiconductor, with the band gap corresponding to the $\Gamma \rightarrow \Gamma$ transition. These results align with earlier DFT studies. Semiconductors with a direct band gap hold great potential for use in solar cells and optoelectronic devices (Nematov, 2024). The energy gap is 0.976 eV in the absence of SOC and drops to 0.934 eV when SOC is included. The impact of SOC on the conduction and valence band regions was significant, leading to shifts in the position of the CBM, as illustrated in Fig. 2 (a) and (b). The CBM shifted downward toward the Fermi level. The variation in the band gap between the two approaches is due to SOC-induced hybridisation.

To gain deeper insight into the band-gap characteristics of Ba_3AsCl_3 , we studied the total and projected density of states (DOS and PDOS). Fig. 3(a) and (b) display the DOS and the PDOS, respectively. The DOS provides a more comprehensive understanding of the electronic characteristics of materials. It outlines how the energy states of electrons are distributed in a material, showing the number of electronic phases per unit energy that electrons can occupy. Conversely, all atoms contribution to the total DOS at the Fermi level is minimal compared to the valence and conduction bands. The PDOS provides a clearer understanding of how different atoms contribute to the electronic behaviour of materials. On the other hand, it illustrates how individual atoms and their orbital contributions affect the material's band gap

energy (Shanto et al., 2023). The PDOS distribution for Ba_3AsCl_3 is shown in Fig. 3(b). The conduction band energy ranges from 0-5eV, with Ba-s, As-s and Cl-s having the most contribution in the conduction band. The Ba-p and Cl-p contribute to the electronic structure of the valence band, while As-p contribution is toward the Fermi level.

Elastic Properties

Elastic properties provide insight into how atoms are bonded and how the material responds to mechanical forces, such as stretching and compression. The elastic constants obtained are shown in Table 2. To ensure that a material is mechanically stable, it must satisfy the Born-Huang criteria defined by the equations below (Jamal et al., 2014).

$$\begin{aligned} C_{11} &> 0 \\ 2C_{12} + C_{11} &> 0 \\ -C_{12} + C_{11} &> 0 \\ C_{44} &> 0 \\ C_{12} = C_{13} = C_{21} = C_{23} = C_{31} = C_{32} \end{aligned}$$

The calculated elastic constants C_{ij} meet the Born-Huang criteria, indicating that Ba_3AsCl_3 is mechanically stable.

Table 2: The calculated elastic constants C_{ij} (GPa), resistance to shear deformation by shear stress C' (GPa), Cauchy pressure C'' (GPa), and Kleinman's parameter (ξ)

Compound	C_{11}	C_{12}	C_{44}	C'	C''	ξ
Ba_3AsCl_3	63.86	8.58	10.95	22.7	-2.37	0.29

Table 3: Calculated Young modulus Y , Shear modulus G , Poisson ratio ν , Bulk modulus B , Hardness H , Machinability index μ_m and Anisotropic factor A

Compound	Y (GPa)			G (GPa)			ν (GPa)			B (GPa)	H	μ_m	A
	Y_V	Y_R	Y_H	G_V	G_R	G_H	ν_V	ν_R	ν_H				
Ba_3AsCl_3	43.43	36.75	40.01	17.62	14.43	16.03	0.232	0.273	0.251	27.01	2.66	2.47	0.39

The parameters are calculated using the equations below (Naheer & Naqib, 2021; Sahafi et al., 2024).

$$\begin{aligned} C' &= \frac{-C_{12} + C_{11}}{2} \\ C'' &= -C_{12} + C_{11} \\ \xi &= \frac{8C_{12} + C_{11}}{2C_{12} + 7C_{11}} \end{aligned}$$

They measure the crystal's stiffness, brittleness, or ductility and bond resistance to stretching and bending. The calculated Cauchy pressure is negative, which indicates the brittleness of Ba_3AsCl_3 . The value of calculated Kleinman's parameter is closer to 0 than 1, which indicates that the mechanical strength in Ba_3AsCl_3 is influenced by bond stretching contribution over bond bending.

Mechanical Properties

The mechanical properties, such as Young modulus, Shear modulus, Poisson ratio and Bulk modulus, are obtained from calculated elastic constants using the Voigt-Reuss-

Hill approximation given by the equations below (Hao et al., 2024; Sahafi et al., 2024).

$$\begin{aligned} B_H &= \frac{-B_R + B_V}{2} \\ G_H &= \frac{-G_R + G_V}{2} \\ Y_H &= \frac{9GB}{(G + 3B)} \\ \nu &= \frac{3B - 2G}{2(G + 3B)} \end{aligned}$$

The bulk modulus of materials is used to estimate the hardness and the resistance to compression. Materials with high bulk modulus are harder and more resistant to compression. Young's modulus measures a material's stiffness, that is, how it stretches or compresses under uniaxial stress, and the shear modulus measures a material's resistance to deformation. The findings suggest

that Ba_3AsCl_3 has moderate values for all the moduli calculated (Shear, Young and Bulk), highlighting its potential for application in flexible optoelectronics. Poisson's ratio is another parameter that indicates a material's brittleness and ductility.

Other mechanical properties, such as hardness H , machinability index μm , and anisotropic factor A , are calculated using the equations below.

$$H = \frac{(1 - 2\nu)Y}{6(1 + \nu)}$$

$$\mu\text{m} = \frac{B}{C_{44}}$$

$$A = \frac{2C_{44}}{C_{11} - C_{12}}$$

A material's capacity to resist permanent deformation is influenced by its hardness. Machinability index refers to how easily a material can be cut, shaped or processed using machine tools. Materials with a high machinability index can be processed easily, whereas those with a low machinability index are harder to machine and require more time and effort (Sarker et al., 2024, 2025). Anisotropy index is a measure of how a material's elastic properties vary with direction. A value of 1 shows an isotropic nature and deviation from this value shows anisotropy. Ba_3AsCl_3 is moderately hard, has a high machinability index and is anisotropic in nature. The computed mechanical properties are in reasonable agreement with previously reported values for similar A_3BX_3 compounds, indicating similar trends in mechanical stability across the family. In this work, we present a comprehensive first-principles study of Ba_3AsCl_3 , in which spin-orbit coupling is explicitly incorporated, revealing its role in determining the structural properties and electronic characteristics, and highlighting its potential for optoelectronic and photovoltaic applications

CONCLUSION

In this study, we investigated the Structural, electronic, elastic, and mechanical characteristics of Ba_3AsCl_3 using density functional theory. The Structural investigation shows that Ba_3AsCl_3 has a stable cubic structure. The electronic study reveals that Ba_3AsCl_3 exhibits a direct band gap of 0.976eV when SOC is not included and 0.934eV when SOC is included, making it a semiconductor. The mechanical properties investigation suggests that Ba_3AsCl_3 is mechanically stable, anisotropic, and slightly brittle in nature. It also has a high machinability index. Overall, our findings indicate that Ba_3AsCl_3 perovskite is mechanically stable with a suitable bandgap and favourable electronic characteristics. Although optical properties are not covered here, the material's direct bandgap suggests potential for efficient optoelectronic and solar cell applications.

ACKNOWLEDGEMENT

The authors acknowledge TETFund through Umaru Musa Yar'adua University, Katsina (UMYUK), Katsina State, Nigeria, for financial support on this research work.

REFERENCES

- Al-Shomar, S. M., Liaqat, M., Anmol, I., Quraishi, A. M., Khan, I., Amina, Arshad, K., Turdialiyev, U., Almahri, A., Tirth, V., Algahtani, A., Alsuhailani, A. M., Abdullah, Refat, M. S., & Zaman, A. (2024). Study of structural, electronic, mechanical, optical and thermoelectric properties of As based halide-perovskites Ba_3AsX_3 (X= F, Cl): A first-principles insights. *Journal of Materials Research and Technology*, 31, 2450–2460. [Crossref]
- Apurba, I. K. G. G., Islam, M. R., Rahman, M. S., Rahman, M. F., & Park, J. (2024). Tuning the physical properties of inorganic novel perovskite materials Ca_3PX_3 (X=I, Br and Cl): Density function theory. *Heliyon*, 10(7). [Crossref]
- Barman, P., Rahman, M. F., Islam, M. R., Hasan, M., Chowdhury, M., Hossain, M. K., Modak, J. K., Ezzine, S., & Amami, M. (2023). Lead-free novel perovskite Ba_3AsI_3 : First-principles insights into its electrical, optical, and mechanical properties. *Heliyon*, 9(11). [Crossref]
- Dal Corso, A. (2014). Pseudopotentials periodic table: From H to Pu. *Computational Materials Science*, 95, 337–350. [Crossref]
- Feng, H.-J., & Zhang, Q. (2021). Predicting efficiencies >25% A_3MX_3 photovoltaic materials and Cu ion implantation modification. *Applied Physics Letters*, 118(11). [Crossref]
- Gayen, D., Chatterjee, R., & Roy, S. (2024). A review on environmental impacts of renewable energy for sustainable development. *International Journal of Environmental Science and Technology*, 21(5), 5285–5310. [Crossref]
- Giannozzi, P., Baroni, S., Bonini, N., Calandra, M., Car, R., Cavazzoni, C., Ceresoli, D., Chiarotti, G. L., Cococcioni, M., Dabo, I., Corso, A. D., Fabris, S., Fratesi, G., de Gironcoli, S., Gebauer, R., Gerstmann, U., Gougoussis, C., Kokalj, A., Lazzeri, M., ... Wentzcovitch, R. M. (2009). Quantum ESPRESSO: a modular and open-source software project for quantum simulations of materials. *Journal of Physics: Condensed Matter*, 21(39), Article 395502. [Crossref]
- Hao, G., Hou, H. J., Zhang, S. R., & Xie, L. H. (2024). Theoretical study on the elastic and thermodynamic properties of CdS. *Chalcogenide Letters*, 21(1), 39–51. [Crossref]
- Harun-Or-Rashid, M., Ferdous Rahman, M., Monirul Islam, M., Mohammed, M. K. A., & Bani-Fwaz, M. Z. (2024). Insight into the structural, electronic, mechanical, and optical properties of Pb-free new inorganic perovskite Mg_3SbX_3 (X = I, Br, Cl, F) via first-principles analysis. *Inorganic Chemistry Communications*, 168. [Crossref]
- Hasan, N., Hasan, M. M., Kabir, A., & Rashid, M. H. (2023). Theoretical study of the structural,

- electronic, mechanical, and optical of transition metal (mn, co, and ni) doped FrGeI_3 perovskites. *Results in Materials*, 20. [\[Crossref\]](#)
- Hummel, R. E. (2000). *Electronic properties of materials* (3rd ed.). Springer.
- Jamal, M., Jalali Asadabadi, S., Ahmad, I., & Rahnamaye Aliabad, H. A. (2014). Elastic constants of cubic crystals. *Computational Materials Science*, 95, 592–599. [\[Crossref\]](#)
- Lawal, A., Shaari, A., Ahmed, R., & Jarkoni, N. (2017). Sb_2Te_3 crystal a potential absorber material for broadband photodetector: A first-principles study. *Results in Physics*, 7, 2302–2310. [\[Crossref\]](#)
- Lawal, A., Shaari, A., Taura, L. S., Radzwan, A., Idris, M. C., & Madugu, M. L. (2021). G0W0 plus BSE calculations of quasiparticle band structure and optical properties of nitrogen-doped antimony trisulfide for near infrared optoelectronic and solar cells application. *Materials Science in Semiconductor Processing*, 124, Article 105592. [\[Crossref\]](#)
- López-Fernández, I., Valli, D., Wang, C. Y., Samanta, S., Okamoto, T., Huang, Y. T., Sun, K., Liu, Y., Chirvony, V. S., Patra, A., Zito, J., De Trizio, L., Gaur, D., Sun, H. T., Xia, Z., Li, X., Zeng, H., Mora-Seró, I., Pradhan, N., ... Polavarapu, L. (2024). Lead-free halide perovskite materials and optoelectronic devices: Progress and prospective. *Advanced Functional Materials*, 34(6). [\[Crossref\]](#)
- Naher, M. I., & Naqib, S. H. (2021). An ab-initio study on structural, elastic, electronic, bonding, thermal, and optical properties of topological Weyl semimetal TaX ($X = \text{P}, \text{As}$). *Scientific Reports*, 11(1). [\[Crossref\]](#)
- Nematov, D. (2024). Analysis of the optical properties and electronic structure of semiconductors of the Cu_2NiXS_4 ($X = \text{Si}, \text{Ge}, \text{Sn}$) family as new promising materials for optoelectronic devices. *Journal of Optics and Photonics Research*, 1(2), 91–97. [\[Crossref\]](#)
- Pecunia, V., Occhipinti, L. G., Chakraborty, A., Pan, Y., & Peng, Y. (2020). Lead-free halide perovskite photovoltaics: Challenges, open questions, and opportunities. *APL Materials*, 8(10). [\[Crossref\]](#)
- Rahman, M. F., Rahman, M., Hossain, M. F., Islam, B., Al Ahmed, S. R., & Irfan, A. (2024). A numerical strategy for achieving efficiency exceeding 32% with a novel lead-free dual-absorber solar cell using Ca_3SbI_3 and Sr_3SbI_3 perovskites. *Advanced Photonics Research*. [\[Crossref\]](#)
- Ravi, V. K., Mondal, B., Nawale, V. V., & Nag, A. (2020). Don't let the lead out: New material chemistry approaches for sustainable lead halide perovskite solar cells. *ACS Omega*, 5(46), 29631–29641. [\[Crossref\]](#)
- Sahafi, M. H., Cholaki, E., & Bashir, A. I. (2024). First-principles calculations to investigate phonon dispersion, mechanical, elastic anisotropy and thermodynamic properties of an actinide-pnictide ceramic at high pressures/temperatures. *Results in Physics*, 58. [\[Crossref\]](#)
- Sarker, M. A., Hasan, M. M., Luna, S. A., Chowdhury, M. I. H., Talukder, M. R., Islam, M. R., & Ahmad, S. (2025). A DFT investigation of structural, electronic, optical, and mechanical properties of lead-free novel InGeX_3 ($X = \text{Cl}, \text{Br}, \text{and I}$) perovskites for potential applications in multijunctional solar cells. *Energy Science and Engineering*, 13(6), 2757–2771. [\[Crossref\]](#)
- Sarker, M. A., Hasan, M. M., Momin, M. A., Irfan, A., Islam, M. R., & Sharif, A. (2024). Band gap engineering in lead free halide cubic perovskites GaGeX_3 ($X = \text{Cl}, \text{Br}, \text{and I}$) based on first-principles calculations. *RSC Advances*, 14(12), 9805–9818. [\[Crossref\]](#)
- Shahzad, U. (2012). The need for renewable energy sources. *ITEE Journal*, 1(3), 16–18. [\[Link\]](#)
- Shanto, M. A. B., Rahman, M. F., Islam, M. R., Ghosh, A., Azzouz-Rached, A., Albalawi, H., & Mahmood, Q. (2023). Investigating how the electronic and optical properties of a novel cubic inorganic halide perovskite, Sr_3NI_3 are affected by strain. *F1000Research*, 12, 1005. [\[Crossref\]](#)
- Ukoba, K., Yoro, K. O., Eterigho-Ikelegbe, O., Ibegbulam, C., & Jen, T. C. (2024). Adaptation of solar energy in the Global South: Prospects, challenges and opportunities. *Heliyon*, 10(7). [\[Crossref\]](#)
- Zhang, L., Mei, L., Wang, K., Lv, Y., Zhang, S., Lian, Y., Liu, X., Ma, Z., Xiao, G., Liu, Q., Zhai, S., Zhang, S., Liu, G., Yuan, L., Guo, B., Chen, Z., Wei, K., Liu, A., Yue, S., ... Ding, L. (2023). Advances in the application of perovskite materials. *Nano-Micro Letters*, 15(1). [\[Crossref\]](#)